CHAPTER III

RESULTS AND DISCUSSION

3.1 Synthesis, photophysical and photochemical properties of *trans*-cinnamates.

3.1.1 Synthesis of *trans*-cinnamates

The *trans*-cinnamic acids were successfully synthesized using Knoevenagel-Doebner condensation between substituted methoxybenzaldehyde and malonic acid. The structure of all *trans*-methoxycinnamic acids (**1A-10A**, see chapter II, Figure 2.4) were well characterized using ^{1}H-NMR, ^{13}C-NMR, MS and IR. (see appendix A, Figure A1-A12). The *trans*-configurations of C=C double bond of these ten cinnamic acids were confirmed by ^{1}H-NMR (two signals at approximately 6.4 and 8.0 ppm with coupling constant; J=16 Hz, see appendix A). *Trans*-cinnamates were then prepared by esterification between *trans*-cinnamoyl chloride which was prepared *in situ* from cinnamic acids and oxalylchloride, and 2-ethylhexanol. Successful esterifications of these cinnamic acids were confirmed using ^{1}H-NMR and IR; NMR: disappearance of methylene proton adjacent to hydroxyl group (3.6 ppm) of the alcohol and appearance of the doublet of doublet signal of $-CH_2$-O-C- at 4.2 ppm, IR: disappearance of the broad O-H stretching around 3400-2800 cm^{-1}. The *trans*-configuration of the double bond of the cinnamic moiety in the ester was confirmed by ^{1}H-NMR (two signals at ~6.4 and 8.0 ppm, J=16 Hz).

3.1.2 Absorption spectroscopy

Absorption spectra of ten 2-ethylhexyl-*trans*-substituted cinnamates in methanol (Figure 3.1) indicate UVA absorption properties of some cinnamates. Among ten cinnamates, five cinnamates, **5E**, **6E**, **7E**, **9E** and **10E**, show absorption in UVA region. **6E** and **9E** showed absorption in the mid of UVA (~350 nm). Molar absorption coefficient values indicate that **9E** (ε_{348nm}= 14,200 $M^{-1}cm^{-1}$) is two times more efficient in absorbing the mid UVA radiation than **6E** (ε_{352nm} = 6,700 $M^{-1}cm^{-1}$). **5E**, **7E** and **10E** possess high molar absorption coefficients at their UVA absorption maxima (ε_{320} of 19000, 15400, 22400 and M^{-1} cm^{-1} for **5E**, **7E** and **10E**, respectively). However, absorption maxima of **5E**, **7E** and **10E** are too close to the UVB region (Figure 3.1). **1E** and **2E** show intense absorption band at short wavelengths with a shoulder of low extinction coefficient in the UVA region whereas **3E** and **8E** display

a single UVB absorption band. Thus **9E** shows the best UVA absorption property. Since choices of organic UVA in the market are very limited, study of photostability and toxicology of **9E** has been carried out.

3.1.3 Fluorescence spectroscopy.

The fluorescence emission spectra of **1E-10E** in methanol are showed in Figure 3.1. All cinnamates display single emission band with no vibrational structures in this polar solvent. The fluorescence quantum yields (ϕ_f) of these ten cinnamates were determined in methanol (table 3.1). The order of fluorescence intensities of ten cinnamates are **3E, 5E, 7E, 8E, 10E** < **1E, 9E** < **6E** < **2E**. As a results, **3E, 5E, 7E, 8E** and **10E** show very weak fluorescence while **1E** and **9E** show moderate fluorescence (Table 3.1). **6E** emits quite strong fluorescence and **2E** gives the strongest emission. The fluorescence emission maxima of **4E** and **5E** are similar to that of **8E** (ca. 445 nm) indicating similar stabilization of the relaxed Franck-Condon state among the three compounds. **6E, 9E** and **10E** show slightly red shifts

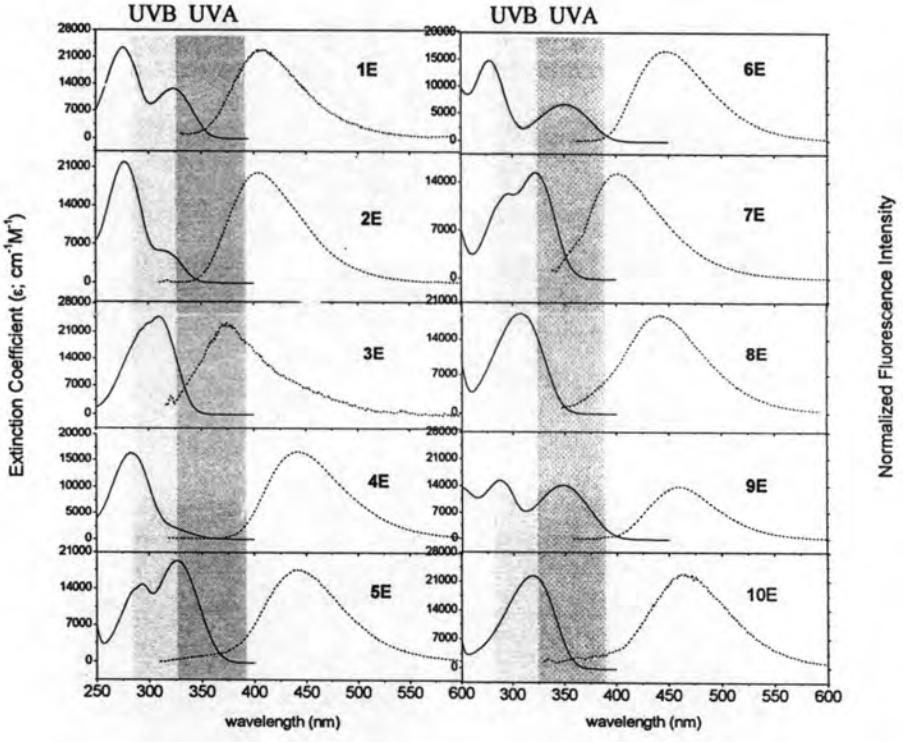

Figure 3.1 Absorption (solid line) and emission (dashed line) spectra of ten 2-ethylhexyl-*trans*-substituted cinnamates in methanol.

(ca. 460 nm) when compared to **8E**. The blue shifts in emission maxima of **1E**, **2E** and **7E** were observed. The singlet fluorescence lifetimes (τ_f) of these ten *trans*-cinnamates were observed in polar solvent. It was found that 2,5-dimethoxy substituted cinnamate **(6E)** and 2,3-Dimethoxy substituted cinnamate **4E** gave the long singlet lifetime (4.8 and 4.4 ns, respectively). The ortho-methoxy substituted cinnamate, **1E**, showed a short singlet lifetime (0.08 ns). As a result, methoxy substituted at meta position might be responsible for the high fluorescence quantum yield and long singlet lifetime of **4E**, **6E** and **2E**. In contrast, para-substituted by methoxy group might be responsible for the very weak fluorescence and very short singlet lifetime of **3E**.

Table 3.1 Photophysical properties of *trans*-**1E** to *trans*-**10E** in methanol.

No.	Abs λ_{max} (nm)	ε ($M^{-1}cm^{-1}$)	Em λ_{max} (nm)	ϕ_f	$\langle\tau\rangle_f$[b]
trans-**1E**	276 323	18 100 11 400	405	0.013	0.08
trans-**2E**	278 319	21 600 7 000	409	0.311	2.51
trans-**3E**	309	24 700	375	6.0×10^{-4}	<0.01[c]
trans-**4E**	283	16 300	442[a]	0.028[a]	4.42[a]
trans-**5E**	292 327	14 654 19 300	443[a]	2.3×10^{-3}[a]	<0.01[c]
trans-**6E**	277 352	15 400 6 700	459[a]	0.174[a]	4.80[a]
trans-**7E**	294 322	8 700 15 400	402[a]	2.0×10^{-3}[a]	<0.01[c]
trans-**8E**	307	18 800	445[a]	2.7×10^{-3}[a]	<0.01[c]
trans -**9E**	290 348	12 400 14 200	461	0.046	0.34
trans-**10E**	320	22 400	463	0.009	<0.01

[a]in acetonitrile. [b]Quinine sulfate is used as fluorescence standard (ϕ_f =0.55 in 0.5M H_2SO_4)[40]. [c]Average fluorescence lifetime calculated by $\tau_f = (\alpha_1\tau_1^2 + \alpha_2\tau_2^2)/(\alpha_1\tau_1+\alpha_2\tau_2)$ where τ_1 and τ_2 are fluorescence lifetimes and α_1 and α_2 are pre-exponential factors of components 1 and 2 deduced from bi-exponential fitting, respectively. [d]Time-resolution of the instrument is about 10 ps.

3.1.4 Photostability of *trans*-cinnamates.

Photostability of all ten 2-ethylhexyl-*trans*-substituted cinnamates were monitored in methanol under simultaneous UVA and UVB exposure (Figure 3.2). Concentration of all *trans*-cinnamates were low ($\sim 10^{-5}$ M) to prevent dimer formation.[26,39] The decrease in absorption was recorded at the absorption maximum wavelength (in the parenthesis). Among five UVA absorbing cinnamates (**5E**, **6E**, **7E**, **9E** and **10E**), **9E** shows the most photostability. Although **5E-8E** are more photostable than **3E** (commercial UVB filter), their extinction coefficients are smaller than **3E**'s. In contrast, although **10E** possesses high molar absorption coefficient, it is the least photostable compound among the ten cinnamates. In addition its absorption band lies too close to the UVB region to be an interesting UVA filter. ^{1}H NMR analyses indicate only cis-isomer formation. Thus, the *cis*-isomer is responsible for the decrease in UV absorption properties. This agrees well with previous study which indicated that the *cis*-**3E** possessed only half the molar absorption coefficient of the trans's.[16-17]

Because among ten cinnamates **9E** and **10E** showed the most and the least photostability in solution, respectively, these two compounds were chosen for further study the photophysical pathway. In addition, photophysical characterization of **3E** (a commercial UVB filter), **1E** (ortho-mono-substituted cinnamate) and **2E** (meta-mono-substituted cinnamate) were carried out. Also *cis*-isomers of these five cinnamates were prepared and purified before subjected to photophysical property characterization. The five *cis*-cinnamates are designated *cis*-**1E**, *cis*-**2E**, *cis*-**3E**, *cis*-**9E** and *cis*-**10E**, and for their corresponding *trans* configuration **1E**, **2E**, **3E**, **9E** and **10E**, respectively.

3.2 Photophysical properties of selected cinnamates

Cis-isomers of the five selected cinnamates were prepared by irradiating the *trans*-isomers with UV light and the obtained *cis-trans* mixtures were then isolated by column chromatography. Structures and purities of *cis*-cinnamates were confirmed by ^{1}H NMR and MS; ^{1}H-NMR: -C**H**=C**H**-Ph showed the signals at 7.2 and 5.8 ppm with J=12 Hz, MS: same molecular weight as *trans*-cinnamate (see appendix A, Figure A15-A22, A33-A35).

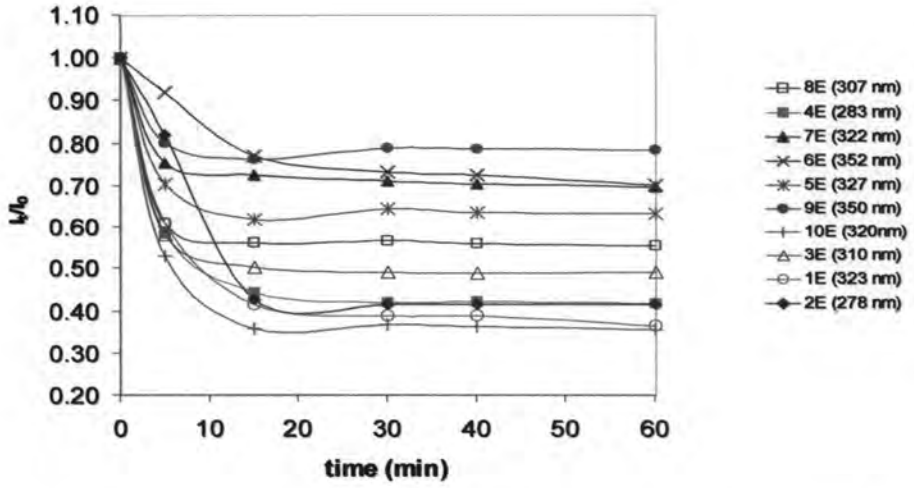

Figure 3.2 Photostability test of ten cinnamates in methanol irradiated by 5.8 mW/cm^2 UVA and 0.47 mW/cm^2 UVB.

3.2.1 Absorption Spectroscopy

The absorption spectra of the five selected (**1E**, **2E**, **3E**, **9E**, and **10E**) cinnamates were measured in hexane, acetronitrile (ACN), dimethylsulfoxide (DMSO), tetrahydrofuran (THF), dichloromethane (DCM) and methanol (Figure 3.3 to 3.7). The spectrum of the *para*-substituted compound (**3E**) shows only single intense absorption band whereas the spectra of **1E, 2E** and **9E** are more complex. The absorption spectra of **1E** and **2E** show two absorption bands, with the band splitting being greater for **1E** than for **2E**. The absorption spectra of **1E, 2E** and **9E** show small solvent induced shifts (9 nm) from DMSO to hexane. Larger solvent shifts at the maximum absorption (20 nm) are observed for **3E** and **10E** when changing from DMSO to hexane (see Appendix B, Table B1). Similar to that of **1E** and **2E**, the absorption spectrum of **9E** shows two absorption bands. The spectrum of **10E** resembles that of **3E** which displays single absorption band.

The absorption spectra of all *cis*-isomers show similar shape to those of the *trans*-isomers, but with smaller extinction coefficients and slightly blue shifted absorption maxima e.g. 323 nm of *trans*-**1E** in methanol shift to 313 nm of *cis*-**1E** in hexane (Table 3.2), suggesting that the energy gaps between ground state and excited state of the *cis*-isomers are slightly larger than those of the *trans*-isomer. More vibrational structures of absorption spectra of all *trans* and *cis*-cinnamates were observed in non-polar solvent.[41] However, the absorption spectra of all cinnamates are quite insensitive to variations of solvent polarity.

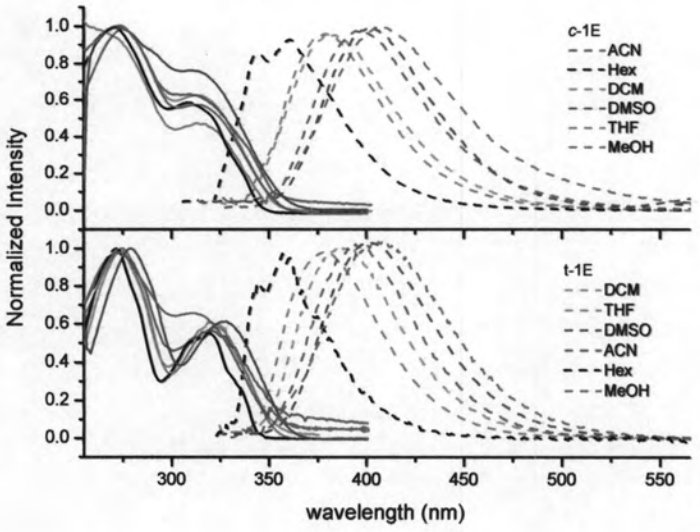

Figure 3.3 Absorption (solid line) and emission spectra (dashed line) of *trans*-**1E** and *cis*-**1E** in variuos solvents.

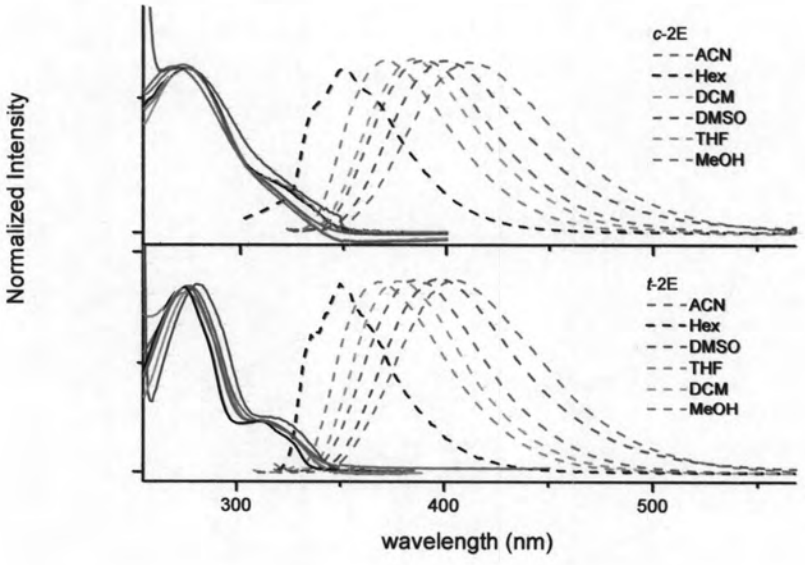

Figure 3.4 Absorption (solid line) and emission spectra (dashed line) of *trans*-**2E** and *cis*-**2E** in various solvents.

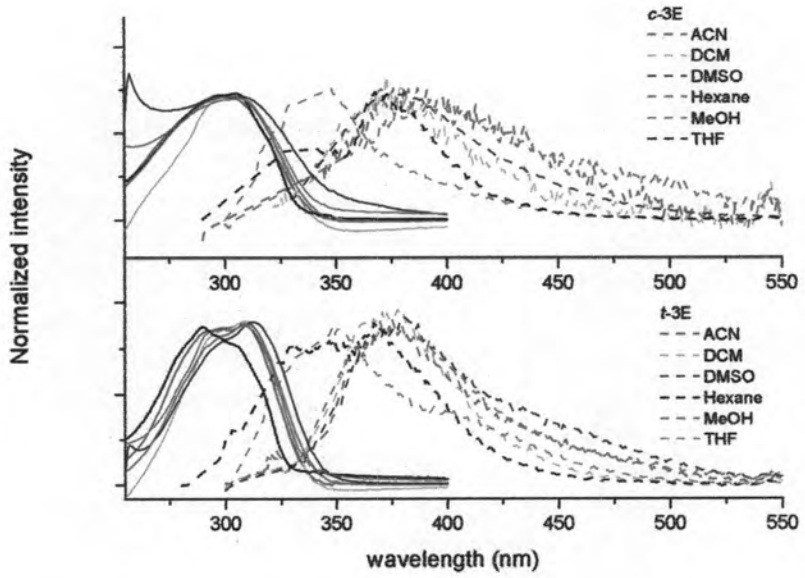

Figure 3.5 Absorption (solid line) and emission spectra (dashed line) of *trans*-**3E** and *cis*-**3E** in various solvents.

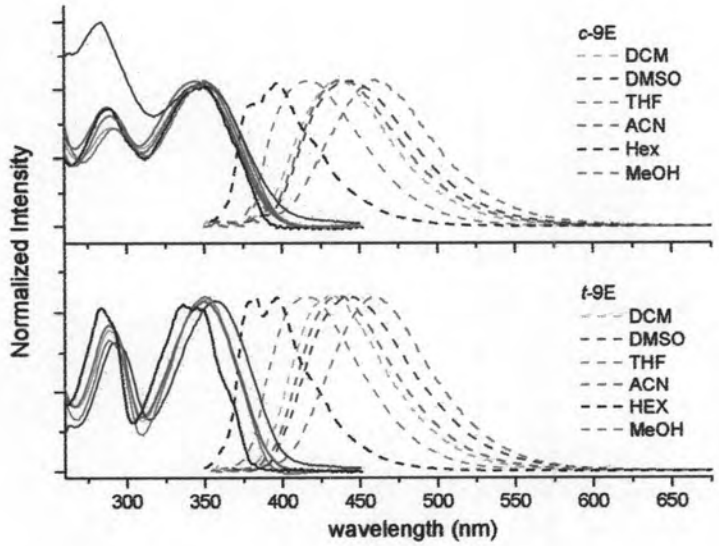

Figure 3.6 Absorption (solid line) and emission spectra (dashed line) of *trans*-**9E** and *cis*-**9E** in various solvents.

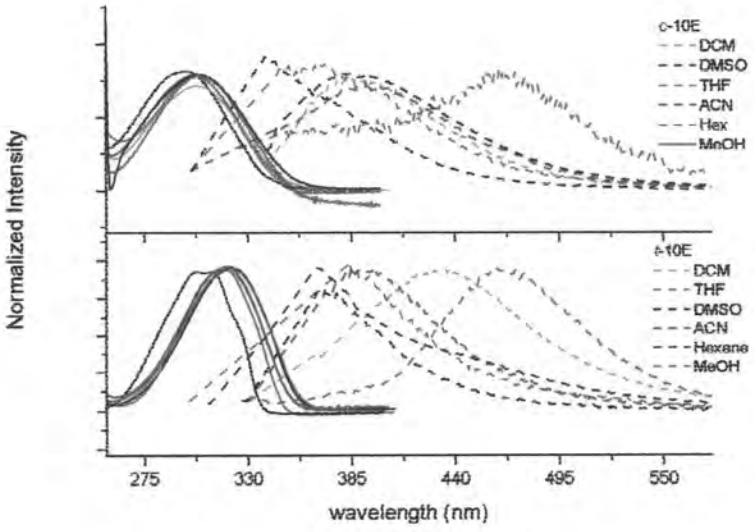

Figure 3.7 Absorption (solid line) and emission spectra (dashed line) of *trans*-**10E** and *cis*-**10E** in various solvents.

Table 3.2 Photophysical properties of *cis*-cinnamates in methanol.

No.	Abs λ_{max} (nm)	ε ($M^{-1}cm^{-1}$)	Em λ_{max} (nm)	ϕ_f	$\langle\tau\rangle_f$[b]
cis-**1E**	271 313	12600 7500	409	4.6×10^{-3}	0.075
cis-**2E**	274 313	11600 3100	410	0.23	2.25
cis-**3E**	303	14100	468	2.0×10^{-4}	<0.01[c]
cis-**9E**	290 345	12100 14000	461	0.01	0.33
cis-**10E**	305	10700	458	3.0×10^{-4}	<0.01

[a]in acetonitrile. [b]Average fluorescence lifetime calculated by $\tau_f = (\alpha_1\tau_1^2 + \alpha_2\tau_2^2)/(\alpha_1\tau_1+\alpha_2\tau_2)$ where τ_1 and τ_2 are fluorescence lifetimes and α_1 and α_2 are pre-exponential factors of components 1 and 2 deduced from bi-exponential fitting, respectively. [c]Time-resolution of the instrument is about 10 ps.

3.3.2 Fluorescence spectroscopy

The fluorescence spectra of the three mono-methoxycinnamates **1E**, **2E** and **3E** and the two trimethoxycinnamates, **9E** and **10E** in various solvents are shown in Figure 3.3-3.7. The spectra of **1E-3E, 9E and 10E** in polar solvents are broad and unstructured. The absorption maxima shift to longer wavelengths upon

increasing the solvent polarity indicated from dielectric constant value from hexane to methanol (Figure 3.3-3.7 and appendix B) indicating that the excited states of these compounds are more stabilized in polar solvent than in non-polar solvent. The shapes and emission maxima of emission spectra of *cis*-**1E**, *cis*-**2E** and *cis*-**9E** are similar to those of the *trans*-isomer at room temperature. This fluorescence probably results from either excitation of traces of *trans*-isomer or isomerization of the *cis*-isomer into the *trans* before emitting. Another possibility is similar lowest excited state of the trans and the cis. Since very weak fluorescence of the *trans* and the *cis*-isomers of **3E** and **10E** were detected in every solvent studied, the emission spectra of these compounds could not be separated from Raman scattering.

Table 3.3 Fluorescence quantum yield of cinnamates in various solvents at room temperature.

Cpds	quantum yield					
	DMSO	**ACN**	**MeOH**	**DCM**	**THF**	**Hexane**
trans-**1E**	9.2×10^{-3}	3.6×10^{-3}	1.3×10^{-2}	4.1×10^{-3}	8.9×10^{-3}	1.0×10^{-2}
cis-**1E**	3.6×10^{-3}	4.4×10^{-3}	4.6×10^{-3}	8.5×10^{-3}	8.2×10^{-3}	3.1×10^{-3}
trans-**2E**	0.04	0.16	0.31	0.20	0.12	0.13
cis-**2E**	0.05	0.03	0.23	0.12	0.05	0.02
trans-**3E**	2.0×10^{-3}	5.2×10^{-4}	6.0×10^{-4}	4.0×10^{-4}	$<1.0\times10^{-3}$	9.3×10^{-4}
cis-**3E**	6.0×10^{-4}	7.8×10^{-4}	2.0×10^{-4}	4.0×10^{-4}	$<1.0\times10^{-3}$	3.3×10^{-4}
trans-**9E**	0.07	0.04	0.05	0.04	0.04	0.04
cis-**9E**	0.06	0.03	0.01	0.04	0.04	0.02
trans-**10E**	1.2×10^{-3}	2.6×10^{-4}	9.2×10^{-3}	3.0×10^{-4}	$<1.0\times10^{-3}$	6.1×10^{-4}
cis-**10E**	9.0×10^{-4}	4.4×10^{-4}	3.0×10^{-4}	3.0×10^{-4}	3.0×10^{-4}	4.0×10^{-4}

The fluorescence quantum yields, ϕ_f, for all cinnamates decrease upon going from polar to nonpolar solvents. Values of ϕ_f for **10E** are similar to those for **3E** which are very small. **2E** shows the largest ϕ_f in every solvent studied. Upon increasing the polarity of the medium, the fluorescence spectra shift to longer

wavelength (Figure 3.3). The solvent-polarity-induced shift can be used to determine the dipole moment of the excited state using Lippert-Mataga equations[42] (equation 2.5 and 2.6), the plots are shown in Figure 3.8 and 3.9 for *trans* and *cis*-isomer, respectively.

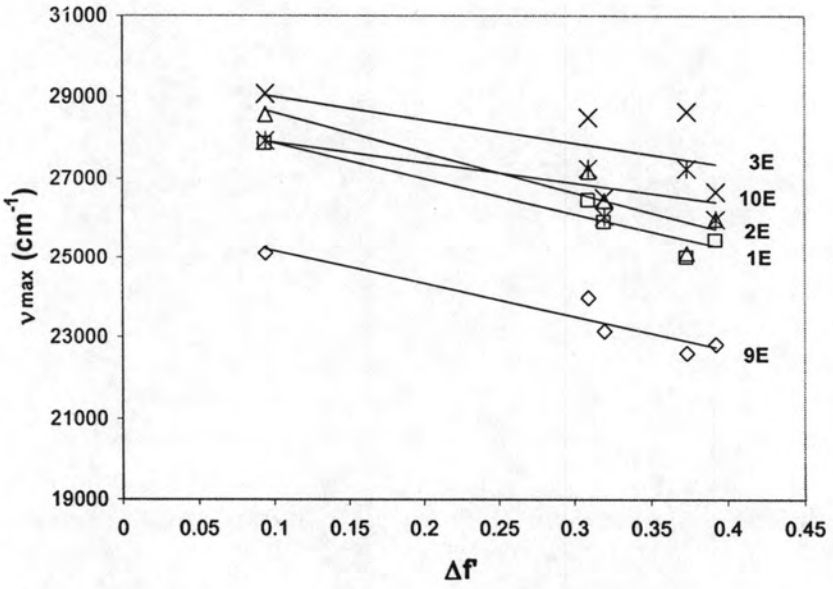

Figure 3.8 Lippert-Mataga plot for *trans*-isomers of cinnamates; □ **1E**, △**2E**, × **3E**, ◇ **9E** and ∗ **10E**.

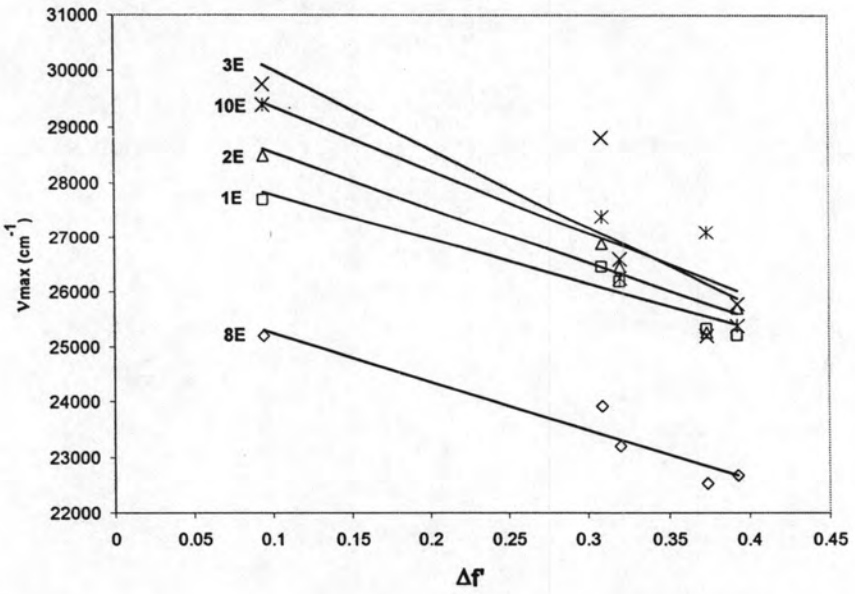

Figure 3.9 Lippert-Mataga plot for *cis*-isomers of cinnamates; □ **1E**, △**2E**, × **3E**, ◇ **9E** and ∗ **10E**.

The ground and excited state dipole moments of *trans*- and *cis*-**1E-3E, 9E and 10E** were calculated using semi-empirical methods PM3 and ZINDO(S). Approximation was done to the molecules in the gas-phase and the results are given in Table 3.4. The predicted excited state dipole moments were larger than the ground state dipole's. The excited state dipole moments of *trans*-**2E** and *cis*-**2E** are larger than those of *trans*-**1E**, *trans*-**2E**, *trans*-**3E** and *cis*-**3E**. Difference between the excited state's dipole moment and ground state's of **2E** is greater than that of **1E** and **3E** and this may cause more excited state stabilization in **2E**. Similar behavior can be seen in **9E** and **10E**. Dipole moment difference between excited state and ground state is more pronounced **9E** compared to **10E**.

Table 3.4 Calculated ground and excited state dipole moments of cinnamates.

	trans				*cis*			
	Sovatochromic slope (cm^{-1})	S_0 (μ/D)	Exp.[a] μ_e/D	Cal. S_3 ($\pi\pi^*$) μ_e/D	Solvatochromic slove (cm^{-1})	S_0 (μ/D)	Exp. μ_e/D	Cal. S_3 ($\pi\pi^*$) μ_e/D
1E	-9024	2.2	12.0	6.3	-8191	2.0	11.5	3.8
2E	-9041	3.2	18.5	10.1	-9800	0.7	15.3	4.1
3E	-2802	3.9	13.0	6.9	-7428	0.3	12.0	3.7
9E	-8144	5.4	15.2	10.4	-8753	3.5	11.7	9.2
10E	-5037	5.4	13.3	12.3	-11405	4.8	13.8	15.0

[a]from Lippert-Mataga equation (equation 2.5 and 2.6, chapter II)

3.3.3 Singlet Fluorescence lifetimes

The singlet fluorescence lifetimes (τ) of all cinnamates were done in methanol, DMSO and hexane. The fluorescence decays of all cinnamates were bi-exponential presumably signaling the contribution from *cis* and *trans* isomer. The τ and percent fraction intensity (%F) including average fluorescence lifetime, $\langle\tau\rangle_f$ of each component are shown in Table 3.5. The τ of all cinnamates are shorter when the polarity of the solvents is decreased. The meta-substituted compound (**2E**) has long fluorescence lifetimes (2.51 and 2.25 ns for *trans* and *cis*-isomer in methanol, respectively). The lifetime of **3E** and **5E** are too short to be resolved from the instrument response function; thus their lifetimes should be less than 10 ps.

Table 3.5 Fluorescence lifetimes of cinnamates in methanol, DMSO and hexane.

Cpds	MeOH				DMSO				Hexane			
	τ (ns)	%F[a]	$<\nu_f$	X^{2b}	τ (ns)	%F	$<\nu_f$	X^2	τ (ns)	%F	$<\nu_f$	X^2
trans-**1E**	τ_1 0.1 τ_2 0.1	28.4 71.6	0.082	1.3	τ_1 0.2 τ_2 0.1	88.0 12.0	0.2	1.1	τ_1 0.7 τ_2 0.1	7.1 92.9	0.13	1.9
cis-**1E**	τ_1 0.1 τ_2 0.04	55.3 44.7	0.075	1.5	τ_1 0.2 τ_2 0.1	76.6 23.4	0.2	1.2	τ_1 1.1 τ_2 0.1	8.5 91.5	0.17	1.3
trans-**2E**	τ_1 2.6 τ_2 0.6	96.0 4.0	2.51	1.7	τ_1 1.3 τ_2 0.4	81.5 18.5	1.1	1.4	τ_1 1.7 τ_2 0.6	64.4 35.6	1.32	1.3
cis-**2E**	τ_1 2.3 τ_2 0.1	97.8 2.2	2.25	1.6	τ_1 1.0 τ_2 0.1	93.2 6.8	0.9	1.4	τ_1 2.0 τ_2 0.6	70.6 29.4	1.59	1.7
trans-**9E**	τ_1 0.3 τ_2 0.06	94.2 5.8	0.33	1.1	τ_1 0.6 τ_2 0.03	76.5 23.5	0.5	1.4	τ_1 0.3 τ_2 0.02	68.7 31.3	0.23	1.2
cis-**9E**	τ_1 0.4 τ_2 0.6	90.6 9.4	0.33	1.1	τ_1 0.4 τ_2 0.01	95.2 4.8	0.4	1.3	τ_1 0.2 τ_2 0.1	91.4 8.6	0.22	0.9

[a]fraction intensity of the fluorescence lifetime of the fist (τ_1) and the second component (τ_2), [b]Least-Square.

The radiative rate constants of all cinnamates in methanol and hexane (Table 3.6) have been calculated using the Strickler-Berg relationship[43] (equation 3.1).

$$k_f = 2.88 \times 10^{-9}\, n^2\, \tilde{\nu}^2 \int \varepsilon(\tilde{\nu})\, d\tilde{\nu} \qquad (3.1)$$

where $\varepsilon(\nu)$ is the molar absorption spectrum on a wavenumber (cm^{-1}) scale, n is the refractive index of the solvent, and ν is the mean transition energy between absorption and emission spectra (see appendix B, Figure B1-B10 and Table B2 and B3).

The experimental ($k_f = \phi_f/\tau$) and calculated radiative rate constants (equation 3.1) for all cinnamates are shown in Table 3.6. The calculated radiative rate constants of *trans* and *cis*-**2E** show slowest relaxation to the ground state. Moreover, it can be seen that *cis*-**1E**, *cis*-**2E** and *cis*-**9E** relax to the ground state *via* fluorescence emission more slowly than the corresponding *trans*-isomers. This agrees well with the lower extinction coefficient at longer wavelength of the cis comparing to the trans. For this reason, *trans*-**2E** relaxes to ground state via fluorescence emission more slowly than

trans-**1E**. The discrepancies between experimental and calculated radiative rate constants may stem from possible non-radiative decay, i.e. the major deactivation pathway of **3E** and **10E** are not through fluorescence.

Table 3.6 Measured and calculated fluorescence rate constant (k_f) of cinnamates in methanol and hexane.

Cpds	k_f (x10^7 s^{-1})			
	MeOH		Hexane	
	Exp.	Cal.[a]	Exp.	Cal.[a]
trans-**1E**	15.6	16.9	7.6	10.7
cis-**1E**	6.1	6.9	1.9	6.17
trans-**2E**	12.3	3.3	9.6	3.3
cis-**2E**	10.2	1.4	1.3	1.6
trans-**3E**	>6.0[b]	17.7	>9.3[b]	21.4
cis-**3E**	>2.0[b]	20.9	>3.3[b]	14.2
trans-**9E**	14.0	21.1	16.3	15.5
cis-**9E**	19.6	22.8	9.45	10.9
trans-**10E**	>9.0[b]	20.0	>6.1[b]	17.2
cis-**10E**	>3.0[b]	25.9	>4.0[b]	17.2

[a]Calculated using Strickler-Berg equation (3.1), [b]fluorescence lifetime both trans and cis of para are shorter than 10 ps which is the instrument limitation

3.3.4 Temperature dependence

Similar positions and similar shapes of the emission spectra of *trans*- and *cis*-isomer of cinnamates are probably caused by the formation of the *cis*-isomer at the excited state during measurements. Thus *trans*-isomer fluorescence upon excitation of the *cis* isomer could be observed. To avoid observation of the emission from the *trans*-isomer, the fluorescence spectra of all five cinnamates were acquired at low temperatures in polar medium, EPA (diethyl ether:iso-propanol:ethanol 5:5:2) and non-polar medium, 3-methylpentane (3MP). The low temperature should help preventing cis-trans photoisomerization during the measurement.

The fluorescence spectra of trans and cis of **1E**, **2E**, **3E**, **9E** and **10E** in EPA at different temperatures are shown in Figure 3.10. The measurement was started at 80K then heated up to 300K. These *trans* and *cis*-cinnamates showed slightly red shift (2-3 nm) when temperature was dropped from 300 to 200 K. Below 200 K, the fluorescence maxima of these cinnamates shifted substantially to shorter wavelengths and revealed more structures relative to those at 300K which resemble their room temperature spectra in nonpolar solvent (Figure 3.3 to 3.7). This behavior is consistent with the temperature dependence of the dielectric constant of EPA; the dielectric constant of EPA usually dropps near the glass transition temperature of the solvent.[44] As a result, the fluorescence spectra of *trans*-**1E**, *trans*-**2E** and *trans*-**9E** were identical to those of their corresponding *cis*-**1E**, *cis*-**2E** and *cis*-**3E** emission. This suggests that 1) cis-trans photoisomerization of these cinnamates may occur in EPA glass[45] or 2) Franck-Condon state of both isomers are similarly stabilized by polar solvent causing identical fluorescence spectra of the *trans* and the *cis* of **1E**, **2E** and **9E**. In the case of **3E**, the emission of *trans*-**3E** showed a red shift (20 nm) comparing to *cis*-**3E**. The blue shift (25 nm) of *trans*-**10E** comparing to *cis*-**10E** at 100-200 K was observed. The integrated intensity of the fluorescence decreases as the temperature increases, therefore, ϕ_f values were increased (Table 3.7). Quantitative information on the fluorescence quantum yields of *trans*-**1E**, *cis*-**2E** and *trans*-**10E** could not be obtained at 100 K and below because the spectra of these cinnamates contain a significant contribution from the much more strongly fluorescence. The strong increase of fluorescence quantum yield of **1E** (60-fold for trans and 150-fold for cis) and *cis*-**9E** (100-fold) were observed whereas fluorescence quantum yield of *trans*-**2E** and *cis*-**2E** showed 2 and 3-fold increase compared to those at 300 K, respectively.

Similarities between trans and cis fluorescence spectra of **1E**, **2E** and **9E** are may probably be caused by cis-trans photoisomerization which can occur even at low temperature in polar solvent. To proof this, fluorescence spectra of the five cinnamates were acquired in the non-polar solvent, 3-methylpentane (3MP). The non-polar solvent should reduce the degree of trans-cis photoisomerization.[17] The results at different temperatures are shown in Figure 3.11.

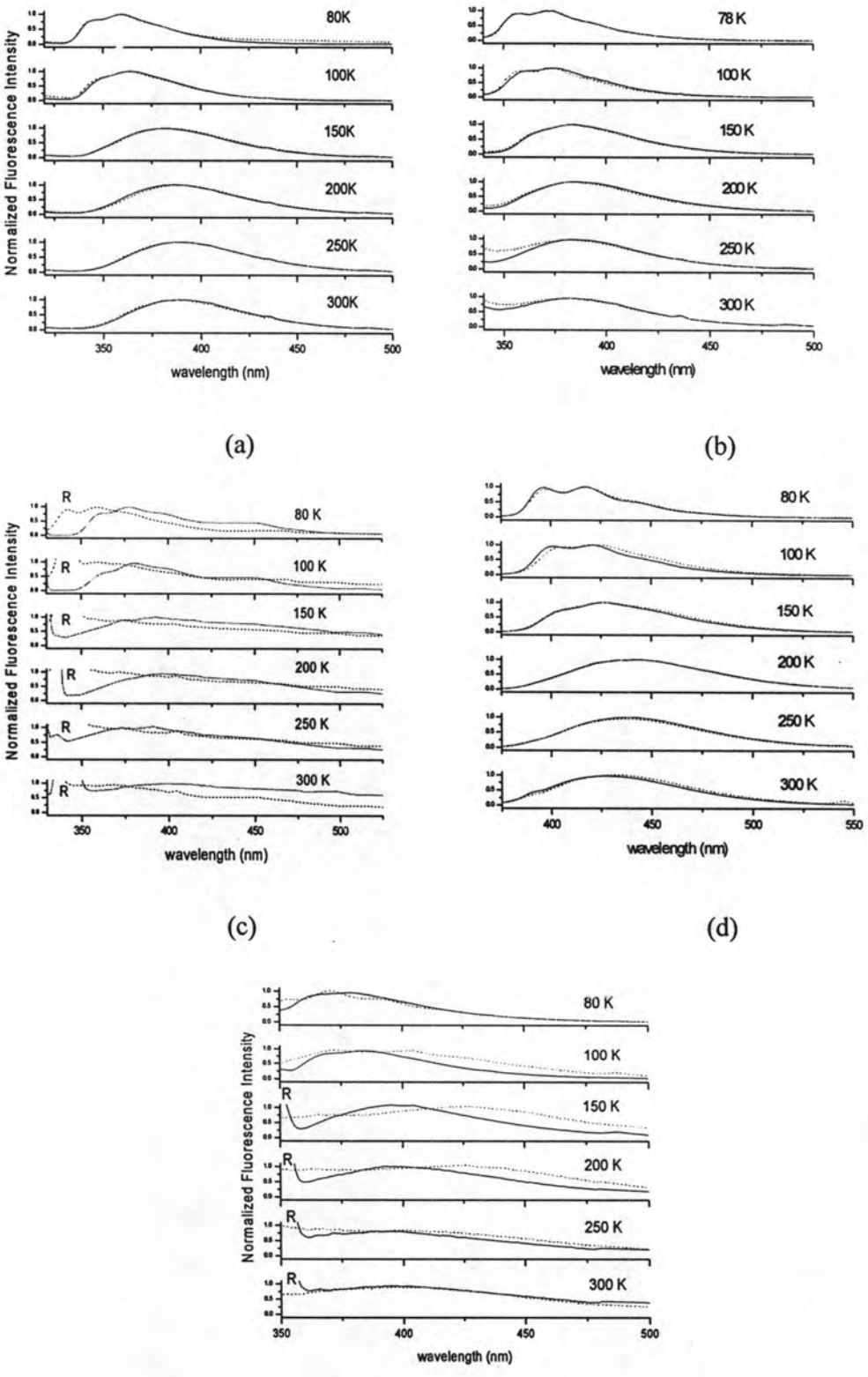

Figure 3.10 Emission spectra of **1E** (a), **2E** (b), 3E (c), **9E** (d) and **10E** (e) *trans*-(solid line) and *cis*-(dashed line) isomer in EPA at different temperature (R = raman scattering).

Table 3.7 Fluorescence quantum yield of cinnamates in EPA[a] at various temperatures

T (K)	% ϕ_f									
	trans-**1E**	*cis*-**1E**	*trans*-**2E**	*cis*-**2E**	*trans*-**3E**	*cis*-**3E**	*trans*-**9E**	*cis*-**9E**	*trans*-**10E**	*cis*-**10E**
300	1.3	0.4	30.1	23.0	0.06	0.02	4.6	0.6	0.9	0.03
250	5.1	0.9	41.5	36.4	0.06	0.02	5.6	1.6	1.1	0.04
200	17.9	5.4	39.4	43.7	0.08	0.05	16.5	7.1	2.9	0.08
150	82.4	19.7	39.1	63.4	0.09	0.07	43.6	12.0	12.9	0.1
100	100	57.4	49.8	100	0.19	1.8	40.7	25.9	69.9	0.3
80	100	61.3	61.6	100	0.91	4.7	40.2	61.5	100	1.3

[a] Fluorescence quantum yield at 300 K of each cinnamate in EPA is that in methanol at room temperature.

Upon raising the temperature from 78 to 297 K, some blue shifts (10-20 nm) of the emission maximum of **1E, 2E** and **9E** were observed. The fluorescence spectra of *trans*-**1E** are identical to those of *cis*-**1E** even in 3MP glass. The singlet lifetimes of *trans*-**1E** and *cis*-**1E** are shown in Table 3.8, using bi-exponential fitting presumably signaling the contribution from cis and *trans*-isomer. It can be seen that the singlet lifetimes of *trans*-**1E** at every temperature studied resemble those of *cis*-**1E**, suggesting that the emission of these two compounds occurs from the same specie which could be the equilibrium of trans and cis at the excited state at low temperature. It can be expected that increasing temperature can cause the torsional distortion of C=C; thus decreasing the amount of the long-lived components. The excitation of *trans*-**1E** and *cis*-**1E** monitored at different emission wavelength at 297 and 78 K were carried out and the results are shown in Figure 3.12. Similarity of the excitation spectra of *trans*-**1E** those of *cis*-**1E** at 279 and 78 K suggests the equilibrium of trans and cis at the excited state during the photoisomerization of **1E** in 3MP glass.

Comparing *trans*-**2E** to *cis*-**2E**, a small red shift (10 nm) was observed at 78 K. Moreover, the emission of *cis*-**2E** displays more blue shift and more structures upon cooling comparing to that of *trans*-**2E** at 78K. However, when the temperature was raised to 297K, the emission from these two isomers became identical (Figure 3.11b). This suggests that photoisomerization of the molecule can occur at room temperature but will be inhibited in 3MP glass. These results are promising to the fluorescence lifetime measurements at 78 K up to room temperature.

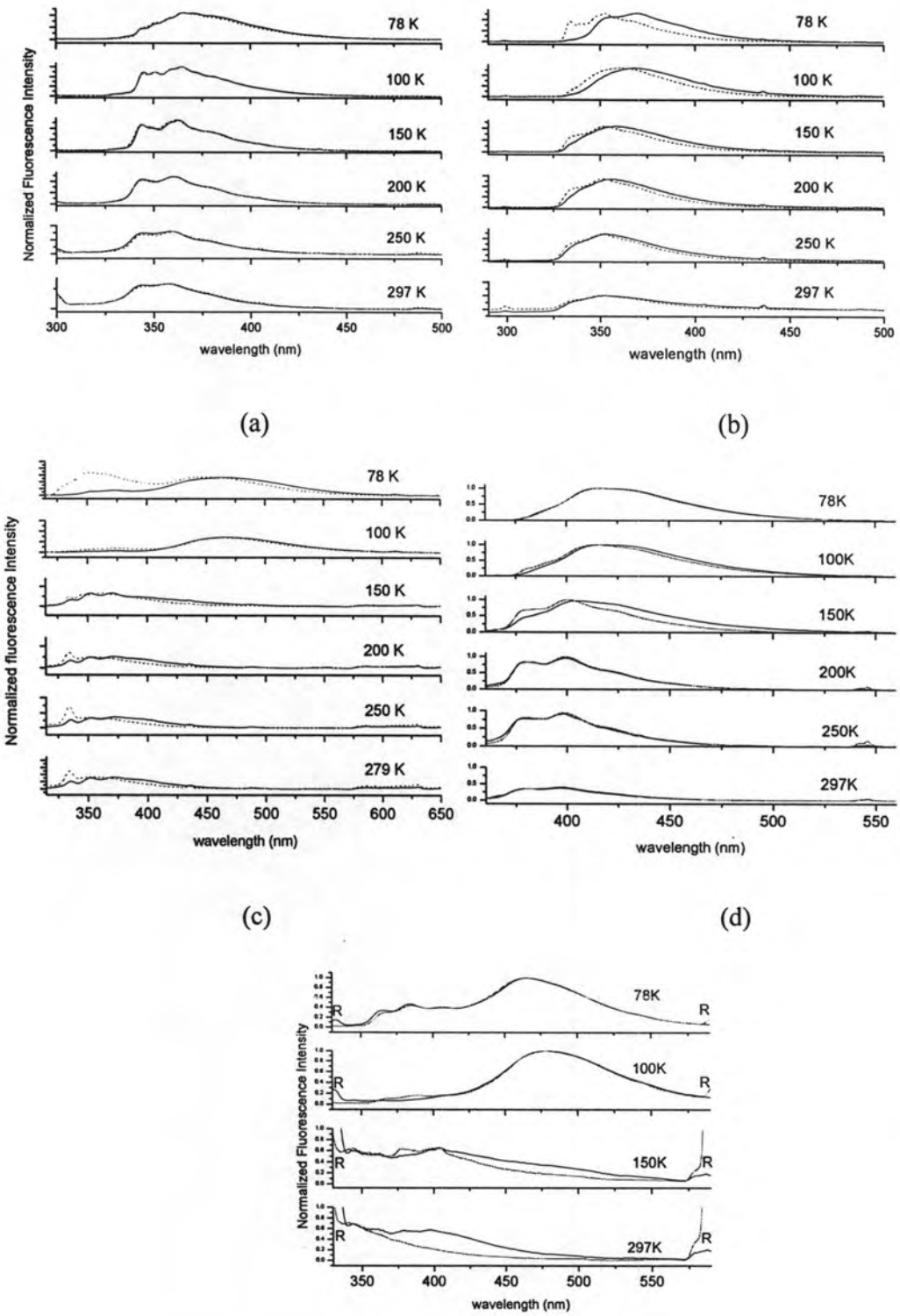

Figure 3.11 Emission spectra of **1E** (a), **2E** (b), **3E** (c), **9E** (d) and **10E** (e) *trans*-(solid line) and *cis*-(dashed line) isomer in EPA at different temperature (R = raman scattering).

Table 3.8 Low temperature singlet lifetimes for *trans* and *cis*-**1E** in 3MP.

T(K)		τ_1 (ns)	%F_1	τ_2 (ns)	%F_2	X^2	$<\tau>_f$ (ns)
297	*trans*	0.1	87.8	1.1	12.2	1.3	0.2
	cis	0.1	70.3	1.1	29.7	1.1	0.4
250	*trans*	0.1	94.5	1.9	5.5	1.0	0.2
	cis	0.2	79.6	2.0	20.4	1.4	0.5
200	*trans*	0.6	86.6	1.6	13.4	1.3	0.8
	cis	0.6	72.6	1.3	27.4	1.3	0.7
150	*trans*	0.5	21.0	2.1	79.0	1.4	1.8
	cis	0.7	31.6	2.2	68.5	1.4	1.7
100	*trans*	1.0	37.9	2.6	62.1	1.4	2.0
	cis	0.9	34.1	2.4	65.9	1.2	1.9
78	*trans*	0.8	22.2	2.3	77.8	1.4	1.9
	cis	0.1	8.0	2.1	92.0	1.2	2.0

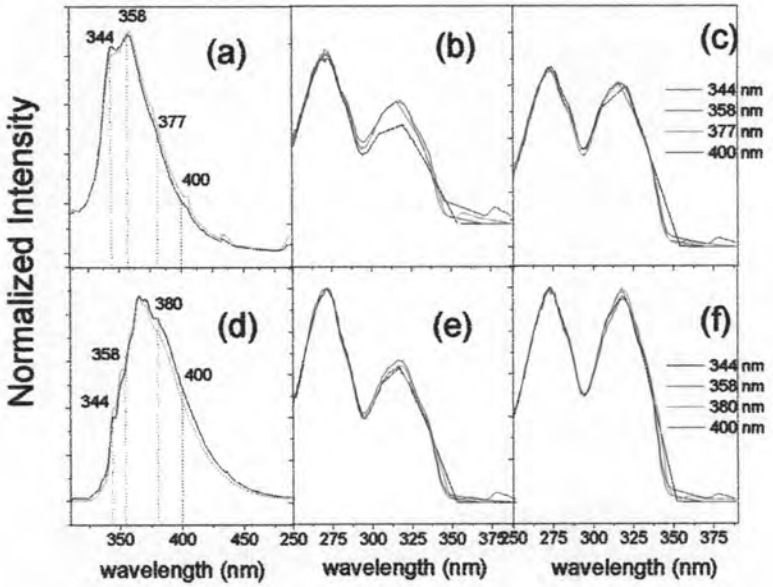

Figure 3.12 Fluorescence spectra of (a) *trans*-**1E** (solid line) and *cis*-**1E** (dashed line) at 297 K; (b) excitation spectra of *trans*-**1E** and *cis*-**1E** (c) at different emission wavelength at 297 K; Fluorescence spectra of (d) *trans*-**1E** (solid line) and *cis*-**1E** (dashed line) at 78 K; (e) excitation spectra of *trans*-**1E** and *cis*-**1E** (f) at different emission wavelength at 78 K.

The $<\tau>_f$ of *trans*-**2E** and *cis*-**2E** slightly increased (1 ns) with increasing temperature from 78 to 150 K and decreased when temperature was raised to 297 K (3 ns) (Table 3.9). Moreover, the fractional intensity (%F) of each component of *trans*-**2E** seems to be constant at all temperatures. The fractional intensity of long-lived

component of *cis*-**2E** decreased from 82% to 50% when the temperature was raised from 78 to 297 K, suggesting that the *cis*-isomer could isomerize to the trans at higher temperature. The excitations of *trans*-**2E** and *cis*-**2E** monitored at different emission wavelengths at 297 and 78 K were done to confirm this assumption (Figure 3.13). At 297 K, the excitation spectra of both isomers were identical at all emission wavelengths. However, at 78K the red shift was observed when the spectra were monitored at longer emission wavelengths. This suggests that the degree of photoisomerization of **2E** could be very slow at 78 K and increased as a function of temperature.

Table 3.9 Low temperature singlet lifetimes for *trans*-**2E** and *cis*-**2E** in 3MP

T(K)		τ_1 (ns)	%F_1	τ_2 (ns)	%F_2	X^2	$<\tau>_f$ (ns)
297	*trans*	1.0	39.6	3.7	60.4	1.1	2.6
	cis	1.1	48.3	4.2	51.7	1.2	2.7
250	*trans*	2.5	47.1	6.6	53.0	1.1	4.7
	cis	1.9	28.9	5.4	71.1	1.2	4.4
200	*trans*	3.5	53.0	7.7	47.0	1.1	5.5
	cis	1.4	12.4	5.6	87.6	1.3	5.0
150	*trans*	2.9	48.2	7.0	51.8	1.0	5.0
	cis	2.1	27.4	5.8	72.7	1.2	4.8
100	*trans*	2.7	44.2	5.3	55.8	1.1	4.2
	cis	1.3	16.6	4.4	83.4	1.3	3.9
78	*trans*	2.6	25.1	5.4	74.9	1.0	4.7
	cis	1.4	17.5	4.5	82.5	1.3	3.9

Table 3.10 Fluorescence quantum yield of cinnamates in 3-methylpentane at various temperatures

Temp (K)	% ϕ_F									
	trans-**1E**	*cis*-**1E**	*trans*-**2E**	*cis*-**2E**	*trans*-**3E**	*cis*-**3E**	*trans*-**9E**	*cis*-**9E**	*trans*-**10E**	*cis*-**10E**
297	0.7	0.6	10.0	2.9	0.03	0.08	2.7	1.2	-[a]	0.04
250	1.9	1.3	31.6	9.2	0.07	0.07	6.5	3.3	-[a]	-[a]
200	5.4	2.4	52.4	17.1	0.09	0.1	14.7	5.9	0.03	-[a]
150	11.8	5.3	63.5	21.8	0.11	0.2	19.9	12.0	0.03	0.1
100	20.8	15.7	72.5	38.0	0.17	0.3	26.7	100	0.03	0.3
78	28.1	51.0	81.8	92.4	0.43	6.9	30.8	100	0.1	1.1

[a] Very weak fluorescence could not isolate from raman scattering.

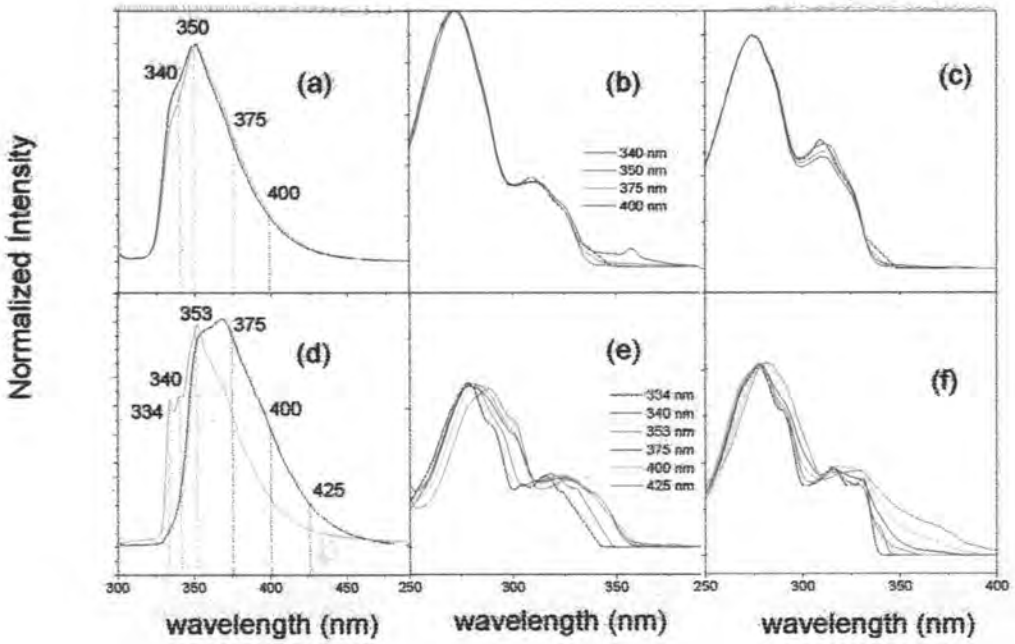

Figure 3.13 Fluorescence spectra of (a) *trans*-**2E** (solid line) and *cis*-**2E** (dashed line) at 297 K; (b) excitation spectra of *trans*-**2E** and *cis*-**2E** (c) at different emission wavelength at 297 K; Fluorescence spectra of (d) *trans*-**2E** (solid line) and *cis*-**2E** (dashed line) at 78 K; (d) excitation spectra of *trans*-**2E** and *cis*-**2E** (f) at different emission wavelength at 78 K.

The fluorescence spectra of *trans*-**3E** show small red shift compaing to the *cis*-isomer's. No change in shape was observed and emissions at 350 nm were very weak even at low temperature. In the case of **10E**, the very weak fluorescence at 297 K was observed and could not be isolated from Raman scattering. Interestingly, at 100 K and below, a new emission band around 460 nm with much longer singlet fluorescence lifetime (42.6, 41.5 ns for *trans*-**3E** and *cis*-**3E**, 35.3, 34.2 ns for *trans*-**10E** and *cis*-**10E**, respectively) was detected in **3E** and **10E**, suggesting π-π interaction between aromatic rings.

3.3.5 Activation Energy Barrier

The activation energy barriers (E_a) for isomerization of the five cinnamates in 3MP can be estimated from the fluorescence quantum yield using equation 3.2 (Table

3.11). The temperature dependence of the non-radiative rate constants fitted to the Arrhenius expression of cinnamates are shown in Figure 3.14. **2E** showed a higher non-radiative activation energy barrier compared to **1E** and **3E**, indicating that **2E** relaxed to the ground state mainly via fluorescence whereas **3E** deactivated to the ground state mainly via non-radiative relaxation.

Electronic excitations of **1E-3E**, **9E** and **10E** have been investigated by calculation using the semiempirical methods PM3 and ZINDO(S). The calculated electronic absorption of cinnamates in the long wavelength absorption band presumably populates the S_2 or S_3 states. The splitting of the S_2-S_3 state energy levels is slightly larger for **1E** and **2E** compared to **3E** (Figure 3.15). Therefore, the absorption spectra of **1E** and **2E** show greater splitting of S_2-S_3 than that of the **3E**. The two bands characteristic of **9E** is similar to **1E** and **2E** (large splitting in the S_2-S_3 energy levels) whereas the single absorption band characteristic of **10E** is similar to that of the **3E**'s (smaller S_2-S_3 energy gap).

$$\ln\left(k_{nr}/k_f\right) = \ln\left(\frac{1}{\phi_f} - 1 - \frac{k_0}{k_f}\right) = \ln\frac{A}{k_f} - \frac{E_a}{RT} \qquad (3.2)$$

Table 3.11. Activation energies for the non-radiative deactivation rate constant based on Arrhenius analysis of the fluorescence quantum yields.

Cpds	In 3-methylpentane	
	E_a (kcal/mol)	A / k_f
trans-**1E**	1.1	380
cis-**1E**	1.0	680[a]
trans-**2E**	1.4	51[b]
cis-**2E**	1.2	140
trans-**3E**	0.4	490[c]
cis-**3E**	0.5	3000[d]
trans-**9E**	1.1	98[a]
cis-**9E**	1.4	630[e]
trans-**10E**	0.4	9000
cis-**10E**	0.7	7400

[a] $k_0/k_f = 2$, [b] $k_0/k_f = 0.2$, [c] $k_0/k_f = 50$, [d] $k_0/k_f = 50$, $T \geq 100$ K, [e] $T \geq 150$ K

This splitting of S_2-S_3 excited singlet state was also observed for *cis*-**1E**, *cis*-**2E** and *cis*-**3E**. Thus, the absorption spectrum of the *cis*-isomer of each cinnamate shows no change in shape relative to that of the *trans*-isomer although the maximum absorption of the cis is slightly blue shifted.

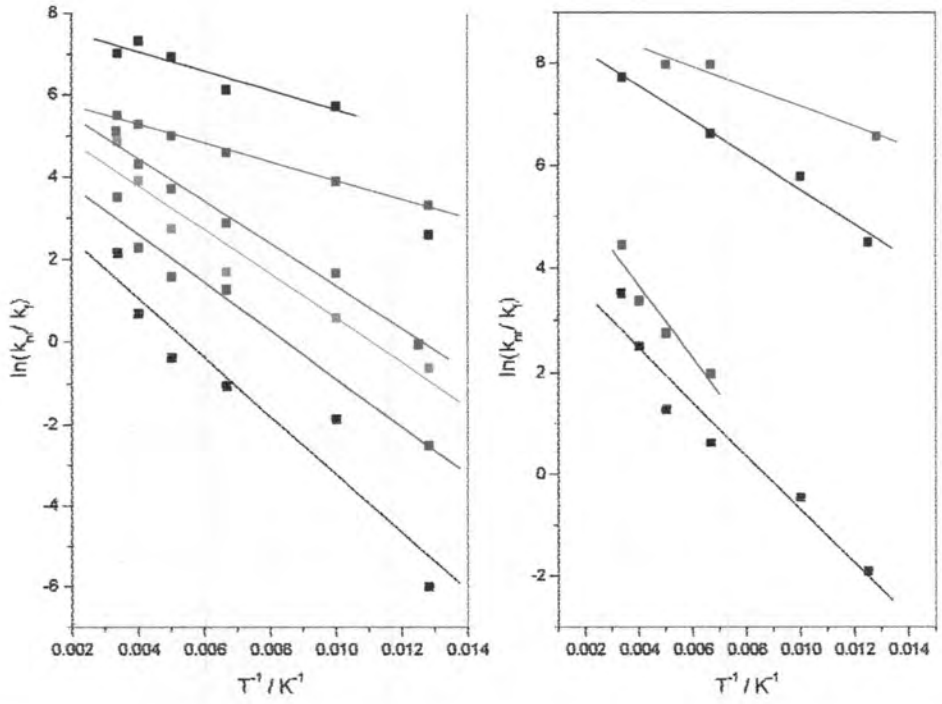

Figure 3.14 The temperature dependence of the non-radiative rate constants fitted top the Arrhenius expression for: **(left)** *trans*-**2E** (black), *cis*-**2E** (red), *trans*-**1E** (cyan), *cis*-**1E** (magenta), *trans*-**3E** (green), *cis*-**3E** (blue); **(right)** *trans*-**9E** (black), *cis*-**9E** (red), *trans*-**10E** (green), *cis*-**10E** (blue). The fitted activation energies are found in Table 3.12.

Table 3.12 Calculated activation barriers estimated from the excited state potential surfaces (following the lowest $\pi\pi^*$ potential surface in each case).

Cpds	E_a / kcalmol^{-1}	
	trans → *cis*	*cis* → *trans*
1E	5.2	3.5
2E	10.0	6.4
3E	3.5	4.9
9E	9.0	9.2
10E	6.5	7.7

3.3.6. Theoretical results

The barriers for torsional distortion in the excited state were estimated from the calculated potential surfaces (Figure 3.15). The theoretical method used is far too simple to give accurate barrier values but is believed to reproduce the trends observed in the experiments. Indeed, the calculated barriers are almost ten times larger than the experimentally observed values but the dominant trends are reproduced, i.e. low barrier for **3E**, larger barrier for **1E**, and largest barrier for **2E**.

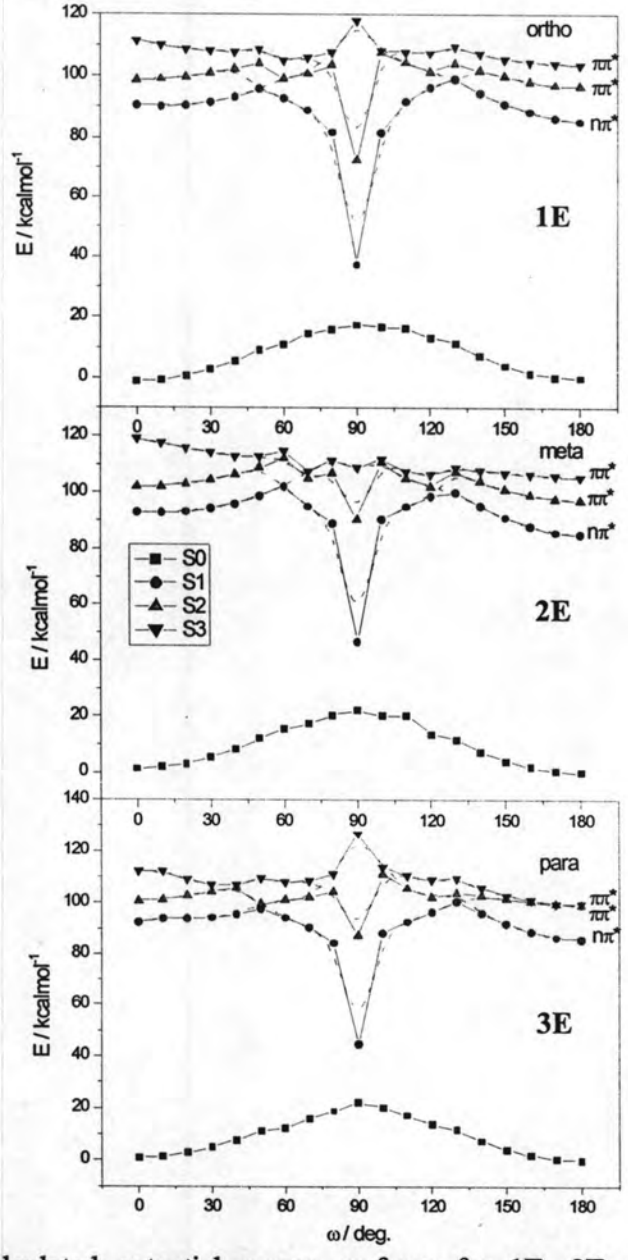

Figure 3.15 Calculated potential energy surfaces for **1E**, **2E** and **3E** (PM3 + ZINDO/S-CI, see text). The approximate adiabatic potential surfaces are shown with dashed lines.

Many approximations were used in the quantum mechanical calculation, the most severe presumably being that the excited state energies were not optimized and the optimized ground state geometries were used with adding vertical excitation energies. This clearly would produce too large barriers. However, the interpretation suggested by these simple calculations was that the splitting between the two lowest excited $\pi\pi^*$ states was dictating the size of the torsional barrier.

The molecules with large predicted state splittings have a large barrier (e.g. **2E**) whereas the molecules with a small predicted state splitting have a small barrier (e.g. **3E**). Extended or through-conjugation is presumably responsible for the smaller barrier of **3E**. The electron-releasing methoxy group can interacted directly to delocalize the charge and stabilize the intermediates. Extended conjugation is not possible for **2E** leading to its high activation energy barrier.[46] This goes well with the empirical observation of state splitting in the UV absorption spectra.

3.4 Preliminary Test

2-Ethylhexyl-2,4,5-trimethoxycinnamate (**9E**) was selected for acute oral toxicity test because of its interesting physical properties and good UVA absorption. The compound was diluted to appropriated concentrations using the mineral oil.

3.4.1 Acute oral toxicity test of 2-ethylhexyl-2,4,5-trimethoxycinnamate (9E)

There was neither death nor any signs of clinical change in rats administered with **9E** at the dosages of 50, 500 and 5,000 mg/kg body weight for the duration of 1, 4, 24 hours and 2-7 days, suggesting that the LD_{50} for **9E** is more than 5,000 mg/kg body weight.

During the seven days of acute toxicity study, there was no significant difference in body weight between the treated and control animals (Fig. 3.16). Pathological examination of rat tissues (liver, kidneys, lung, heart and spleen) collected at the end of the study period revealed no significant difference between the control and the three **9E**-administered groups. No significant pathological change in any tissues could be detected.

The hematological parameters were measured on the first day before the treatment and on the seventh day of the necropsy. All hematological parameters were in the normal values and there was no significant difference among the four groups.

Clinical chemistry evaluation showed that ALT, AST, creatinine, BUN and cholesterol were all in the range of normal clinical chemistry values of the SD rat (Table 3.13). However, the serum ALT values were statistically reduced for all three **9E**-treated groups comparing to the control group. In contrast, creatinine was statistically increased for all three **9E** -treated groups. In addition, the ALT was significantly reduced, this indicated the reducing hepatocellular damage and/or the altering of cell metabolism.

More investigation should be done on this benefit. All animals including the treated and the control rats showed significantly increased creatinine values for the seventh day comparing to the first day of the experiment. However, these creatinine values were in the normal range. This was probable the influence of the growth rate, since the heavily muscle rats will normally produce more creatinine daily than the lightly muscled ones. The BUN values were not differed, this concluded that the renal function was not affected by the chemicals.

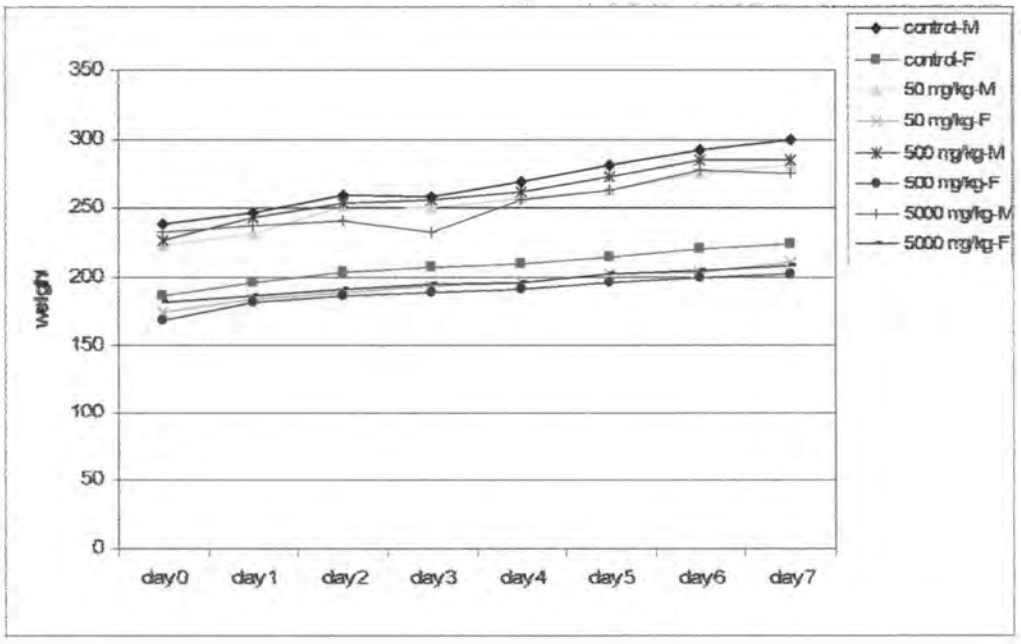

Figure 3.16 The body weight of the **9E** treated and control animals.

Table 3.13 The clinical chemistry (mean ± SD) of the **9E** treated and control animals.

Group	Sex	ALT		AST		CREATININE		BUN		CHOLESTEROL	
		day 0	day 7	day 0	day 7	day 0	day7	day 0	day 7	day 0	day 7
Con - trol	M	33.6±5.9	38.8±8.3	96.96±20.1	83.28±33.9	0.35±0.05	1.12±0.46[a]	15.56±2.7	14.48±1.5	124.42±13.1	124.66±45.3
	F	27.2±5.2	28.4±2.2	80.96±22.5	82.08±32.6	0.3±0.01	1.06±0.52[a]	15.5±2.1	14.4±1.2	126.12±13.4	122.96±12.0
50 mg/kg	M	35.2±3.4	30.4±3.6[a,b]	84±18.3	79.08±11.4	0.29±0.01	1.12±0.33[a]	15.3±2.2	15.46±0.9	114.1±21.3	103.08±8.2
	F	30.4±3.3	23.4±6.5[a,b]	100.64±27.6	63.68±22.5	0.31±0.02	0.9±0.39[a]	16.7±2.8	14.38±1.4	113.08±16.4	124.42±10.3
500 mg/kg	M	29.6±1.7	24.0±4.0[a,b]	96.96±25.8	76.04±27.9	0.33±0.04	1.18±0.47[a]	15.6±1.0	16.82±1.2	128.84±40.2	101.08±12.8
	F	26.0±2.5	19.8±4.3[a,b]	98.24±10.3	77.84±6.4	0.33±0.04	1.12±0.4[a]	16.1±2.4	13.96±1.1	139.36±24.8	134.34±18.1
5000 mg/kg	M	32.8±4.2	26.8±5.4[a,b]	113.36±18.3	74.72±12.9	0.35±0.05	1.12±0.4[a]	14.42±1.4	13.96±0.9	151.08±41.2	110.18±7.5
	F	30.4±1.7	19.6±5.5[a,b]	86.72±18.2	75.2±8.1	0.35±0.05	1.14±0.3[a]	16.24±1.2	12.96±1.8	152.62±31.4	129.06±11.6

[a]significant differences ($P<0.05$) in comparison to the day of treatment

[b]significant differences ($P<0.05$) in comparison to the control